Available online at www.sciencedirect.com
ScienceDirect
Ceramics International 36 (2010) 1621–1628
CERAMICS INTERNATIONAL
www.elsevier.com/locate/ceramint

Effect of A_2O_3 (A = La, Y, Cr, Al) on thermal and crystallization kinetics of borosilicate glass sealants for solid oxide fuel cells

Vishal Kumar, O.P. Pandey, K. Singh *

School of Physics and Materials Science, Thapar University, Patiala 147004, India

Received 10 July 2009; received in revised form 12 January 2010; accepted 20 February 2010
Available online 27 March 2010

Abstract

Influence of various intermediate oxides on thermal, structural and crystallization kinetics of $30BaO–40SiO_2–20B_2O_3–10A_2O_3$ (A = Y, La, Al, Cr) glasses has been studied. The highest glass transition temperature (T_g) with high thermal stability is observed in Y_2O_3 containing glasses as compared to other glasses. The thermal expansion coefficient (TEC) increases with increasing heat treatment duration in all the glasses. The maximum increase in TEC is observed in Cr_2O_3 containing glass ceramics. FTIR study showed that transmission bands due to silicate and borate chains become sharper with splitting after heat treatment. A selected glass sample (BaCr) has been tested for interaction and adhesion with Crofer 22 APU interconnect material for its application as a sealant in solid oxide fuel cell.

Keywords: C. Thermal expansion; D. Glass; D. Glass ceramics; E. Fuel cells; Scanning electron microscopy

1. Introduction

Efforts are being made all over the world to commercialize the solid oxide fuel cell technology due to its higher efficiency and eco friendly nature [1,2]. Based on design, solid oxide fuel cell (SOFC) can be categorized into two main categories namely tubular and planar design. Planar design is better than tubular design due to its higher current density with simple processing [2–7]. However, the planar design of SOFC requires proper sealing at the edges of the cells to prevent fuel leakage and air mixing during cell operation [8,9]. The glass and glass ceramics are considered as most suitable materials for sealant as compared to the conventional sealing materials due to their compatibility with other components of SOFC at high temperature (800–1000 °C) [10]. However, apart from compatibility criteria it should also have good chemical stability in reducing, oxidizing and humid atmosphere. Additionally, sealant should be flexible to withstand a slight compression and expansion in different parts of the stacks.

Many studies have been performed on glass and glass ceramics to achieve above mentioned properties which can make them suitable as a sealant material for SOFC [11,12]. However, each category of glasses has its own drawbacks such as mismatching of thermal expansion due to formation of various crystalline phases during the operation of SOFC. Additionally, interaction among the various components of SOFC may lead to formation of undesirable phases. Some of these phases are very detrimental due to their low thermal expansion. Therefore, based on earlier studies [13–16] on glass and glass ceramics a glass composition $SiO_2–B_2O_3–BaO–A_2O_3$ (A = Y, La, Al, Cr) was selected for the present study. Effect of field strength of intermediate cations on the crystallization kinetics, formation of various crystalline phases and change in thermal properties of the glasses are studied. The structural and thermal properties of these glasses have been characterized using X-ray diffraction, differential thermal analysis (DTA), Thermo gravimetric analysis, and Fourier Transform Infrared Spectroscopy (FTIR). Based on the structural studies the most suitable glass was selected to test the adhesion between glass sealant (BaCr) and Crofer 22 APU (interconnect material).

2. Experimental

Glass composition of $30BaO–40SiO_2–20B_2O_3–10A_2O_3$ (A = Y, La, Al, Cr) (mol%) was prepared by conventional

* Corresponding author. Tel.: +91 1752393130; fax: +91 1752393005.
E-mail address: kusingh@thapar.edu (K. Singh).

0272-8842/$36.00
doi:10.1016/j.ceramint.2010.02.040

splat melt quenching technique. The purity of the constituent oxides were >99.9%. Initially, these oxides were ball milled for 2 h in acetone medium. The ball milled powders were kept in recrystallized alumina crucible for melting at 1550 °C in air. The melt was held at this temperature for 1 h to ensure complete mixing and homogenization of the melt. Finally, the melt was splat quenched using thick copper plates. The glassy nature of the samples was investigated using differential thermal analyzer (DTA). The DTA/TGA measurements were performed with Diamond Pyris TG/DTA (PerkinElmer) using Al_2O_3 powder as reference material in oxygen atmosphere and the average particle size of all glass powders was 20 μm. The DTA curves of all the glasses were taken with different heating rates of 10, 20, 30, 40 °C min^{-1} to calculate the activation energy for crystallization. The temperature and weight loss detection limit are ±1 °C and 0.001 mg respectively during DTA/TGA measurements. The quenched samples were examined to confirm their amorphous nature using X-ray diffraction technique. Furthermore, the X-ray diffraction (XRD) study was also done on heat treated sample to identify various crystalline phases. The XRD were performed using Rigaku model Geiger diffractogram with CuK_α radiation (λ = 1.54 Å) obtained from copper target using an in built Ni filter. The scan speed was 5° min^{-1}. The dilatometer study was performed using Netzsch DIL 402 PC in the temperature range 100–650 °C to determine the thermal expansion coefficient (TEC) of glasses and glass ceramics to study the effect of crystalline phase formation on TEC. Fourier transform infrared (FTIR) spectra were recorded in the range 4000 cm^{-1} to 400 cm^{-1} using a PerkinElmer-Spectrum BX with a spectral resolution of 1 cm^{-1}. 2 mg of each test sample was mixed with 200 mg of KBr in an agate mortar and then pressed into 13 mm diameter pellets. The FTIR spectrum was recorded for these pellets. The scanning electron microscopy (SEM) was done using Hitachi TM 1000 to study the interaction between BaCr glass and APU Crofer sample. For this finely powdered glass was mixed in 2% PVA (poly vinyl alcohol) to form a paste. This paste was applied uniformly over the surface of interconnect. This combination of glass sealant and interconnect was placed in high resistance furnace in air and given a heat treatment for 1 h at a temperature of 1000 °C. The selection of BaCr glass for interaction study at such a high temperature was due to its high melting point as shown in Fig. 1. All other glasses exhibited melting point in the range of 800–850 °C which made them suitable for sealing below 800 °C. After the heat treatment the system was mounted, polished and etched by 2% HF for SEM studies.

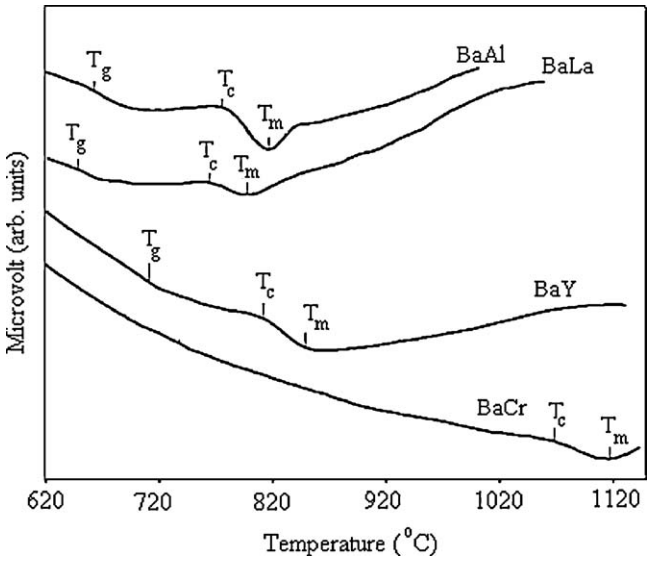

Fig. 1. Differential thermal analysis (DTA) of fine powders of glass samples at 10 °C min^{-1}.

3. Results and discussion

3.1. Differential thermal analysis

Fig. 1 shows the typical DTA curves of all glasses which were used for the present study. The glass transition temperature (T_g), crystallization temperature (T_c) and melting temperature (T_m) of all the glasses are given in Table 1. Apart from this, the glass transition temperature (T_g) obtained by dilatometer is also given in this table. The crystallization peaks were observed to shift towards higher temperature with respect to the increasing heating rate in all the glasses which is because of delay in attaining thermal equilibrium. Ray [17] has reported that T_g is related to the density of covalent cross linking, number and strength of co-ordinate links formed between oxygen atoms and the cations and the oxygen density of network. Higher values of these factors correspond to higher T_g. In case of BaY glass, Y^{3+} might be acting as the network former where it may have higher number of covalent cross linking. The non-bridging oxygen due to modification of glass network by Ba^{2+} might be bonded by Y^{3+} cations which lead to the higher T_g of this particular glass as compared to the BaLa and BaAl glasses. Interestingly, the cation field strength might not be playing very important role to govern the glass transition temperature since the field strength of Al^{3+} has high value as compared to the $Y^{3+}$and La^{3+}cations. Thermal data obtained

Table 1
Glass compositions, transition temperature (T_g), melting (T_m), crystallization temperature (T_c), percentage weight loss 50–1000 °C and activation energy.

Sample name	Composition	T_g (°C) (dilatometer)	T_g (°C) (DTA)	T_c (°C)	T_m (°C)	% Wt. loss 50–1000 (°C)	A.E. (kJ mol^{-1})
BaY	$30BaO–40SiO_2–20B_2O_3–10Y_2O_3$	690	707	810	850	1.25	316
BaLa	$30BaO–40SiO_2–20B_2O_3–10La_2O_3$	656	670	775	815	1.5	303.5
BaAl	$30BaO–40SiO_2–20B_2O_3–10Al_2O_3$	650	664	766	800	1.3	359.54
BaCr	$30BaO–40SiO_2–20B_2O_3–10Cr_2O_3$	–	–	1074	1120	6.5	573.75

from DTA measurement of these glasses was used to calculate the thermal stability and activation energy for crystallization.

The activation energy of all the glasses were calculated using Kissinger equation [18,19]

$$\ln\left(\frac{T_p^2}{\beta}\right) = \left(\frac{E_p}{RT_p}\right) + \text{constant} \quad (1)$$

where β is heating rate and R is gas constant. From the experimental data a graph between $\ln(T_p^2/\beta)$ versus $(1000/T_p)$ was plotted, slope of this graph gives the activation energy of crystallization. The Kissinger plot for activation energy of BaY, BaLa, BaAl and BaCr glasses is shown in Fig. 2. The highest activation energy is observed in BaCr glass followed by BaAl, BaY and BaLa glasses as summarized in Table 1. It is observed that the as prepared BaCr glass exhibit small portion of unreacted crystalline Cr_2O_3 phase which is described in next section.

The presence of microcrystalline Cr_2O_3 phase in glass matrix provides higher strength in local regions, so the formation of new crystalline phase requires higher activation energy as compared to other glasses. On the other hand, higher field strength cation such as Al^{3+} exhibit higher activation for crystallization followed by other cations as Y^{3+} and La^{3+}. The field strength of Al^{3+} which act as intermediate is highest and due to this it holds the glass matrix tightly. Because of this fact it requires higher activation energy for crystallization as compared to the Y^{3+} cation followed by La^{3+} which has the least value of field strength [20]. Moreover, Al_2O_3 addition in glass is well known to prevent the crystallization and control the viscosity of the glasses [21].

3.2. X-ray diffraction for crystallization study

Glass ceramics, as prepared by controlled crystallization of glasses, exhibit superior mechanical properties than glasses and can have various TEC values depending on the type of precipitated crystalline phases and their volume fraction in the glass matrix. Glass ceramics also show higher chemical stability than glasses, especially, under SOFC operating conditions. Therefore, the glasses developed in the present investigation were subjected to long-term heat treatment, namely 10–100 h at 800 °C to study their crystallization behavior and to examine any structural changes that may occur during prolonged thermal operation. All the as prepared glasses were found to be amorphous and exhibited two broad halos in the X-ray diffractogram except BaCr glass in which unreacted Cr_2O_3 phase is present. During heat treatment, glass modifier (Ba) competes with glass intermediates (Y, La, Al, Cr) to enter into the silicate network. Basically, during initial stage of crystallization silica rich phase is formed and in the later stage of heat treatment other cations get added to form the stable crystalline phases [20].

The BaY glass, has the highest glass transition temperature because of higher cross link density and higher field strength of Y^{3+}cation than Ba^{2+} which makes it possible for the modifier (Ba^{2+}) to enter into the glass network and form barium silicate (Ba_2SiO_4) phase instead of yttrium rich phase even after 100 h heat treatment as shown in Fig. 3. It is possible that Y_2O_3 is associated with B_2O_3 instead of SiO_2 network former which may prevent formation of boron and yttria rich crystalline phases in this glass. Our earlier reports [13,14] also indicated that the addition of Y_2O_3 in any glass composition increase the stability of the glasses without forming any detrimental phase during the heat treatment.

In case of BaLa glass (Fig. 4), no significant change is observed after 10 h heat treatment, however at 100 h heat treatment lanthanum boron silicate $LaBO(SiO_4)$ and lanthanum silicate $La_2(Si_2O_7)$ phases are formed. It can be explained on the basis of small size difference between intermediate cation La^{3+}(1.22 Å) and modifier Ba^{2+} (1.43 Å). Therefore, most likely La_2O_3 is acting as glass modifier which leads to lower

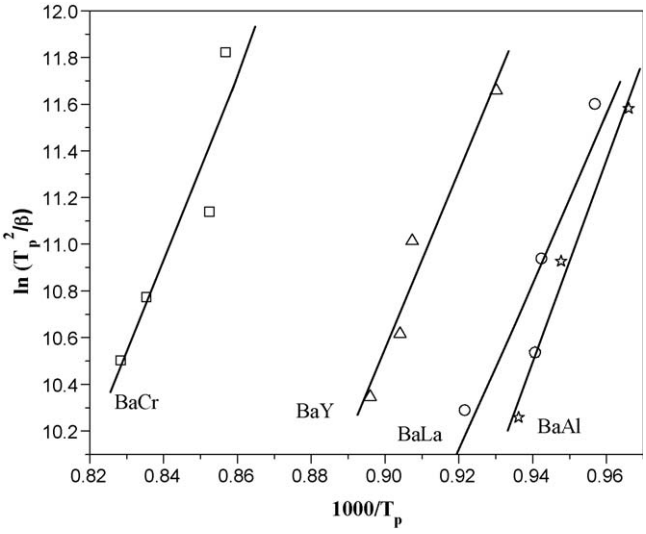

Fig. 2. Kissinger plot of BaY, BaLa, BaAl and BaCr glass samples.

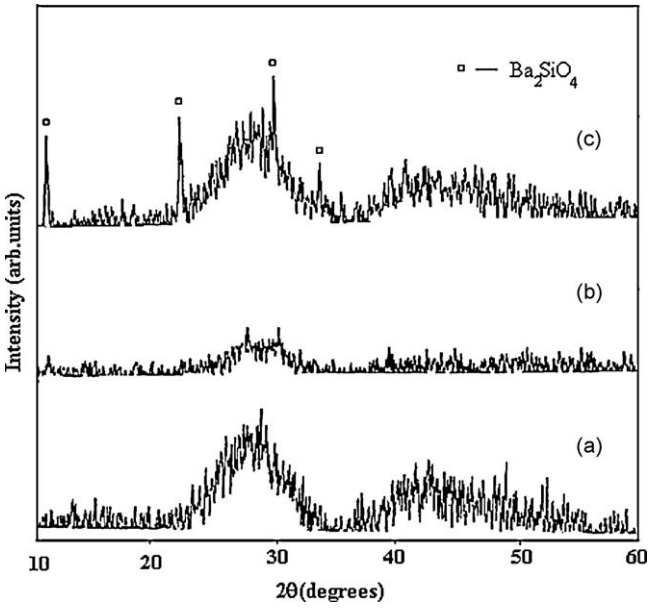

Fig. 3. XRD patterns of BaY glass (a) as prepared, (b) 10 h heat treated and (c) 100 h heat treated at 800 °C.

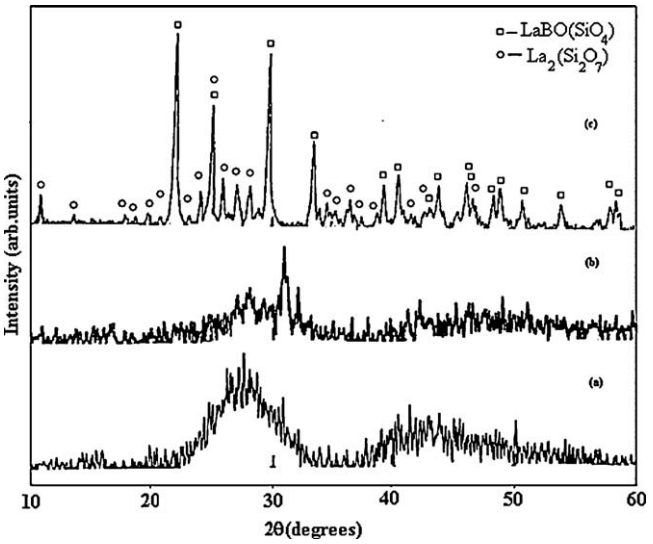

Fig. 4. XRD patterns of BaLa glass (a) as prepared, (b) 10 h heat treated and (c) 100 h heat treated at 800 °C.

activation energy of crystallization with lower glass transition temperature of La_2O_3 containing glass.

The ionic radii of Al^{3+} (0.54 Å) in BaAl glass allow it to fit easily in either tetrahedral or octahedral sites in an oxygen structure. If it is connected as tetrahedrally it works as a network former otherwise it acts as modifier. It is well reported in the literature, that less than 5 mol% Al_2O_3 in glass composition acts as glass former and above that it acts as modifier. Al^{3+} along with Ba^{2+} enters into the glass network and form hexacelsian phase as shown in Fig. 5. The density of hexacelsian phase (3.29 g cm^{-3}) is less than parent BaAl glass (3.5 g cm^{-3}) [15]. However, the difference in densities is not very large to produce appreciable thermal stress in seal during operation for longer duration. TEC of hexacelsian phase is $8 \times 10^{-6}\ K^{-1}$ which lies within the limit required for SOFC application [22]. Moreover, Ghosh et al. [23] have mentioned hexacelsian as a desirable crystalline phase.

On the other hand BaCr glass exhibit unreacted Cr_2O_3 phase as shown in Fig. 6(a). During 100 h heat treatment, barium enters into glass network preferentially and form $BaSi_2O_5$. Conclusively, BaY glass is more stable as compared to BaAl and BaLa samples. In all the samples BaLa and BaAl crystallized fully and did not form any detrimental crystalline phase(s) even after 100 h heat treatment in air.

3.3. FTIR investigation

FTIR transmittance spectra of 100 h heat treated glass ceramics shows the structural rearrangement undergone compared to as prepared glasses shown in Figs. 7–10. All the spectra exhibit three broad transmittance bands i.e. 300–600 cm^{-1}, 600–800 cm^{-1} and 1300–1500 cm^{-1}.

These diffused bands are indicative of the general disorder in the silicate network mainly due to a wide distribution of Q_n units (polymerization in the glass structure, where n denotes the number of bridging oxygen) occurring in these glasses.

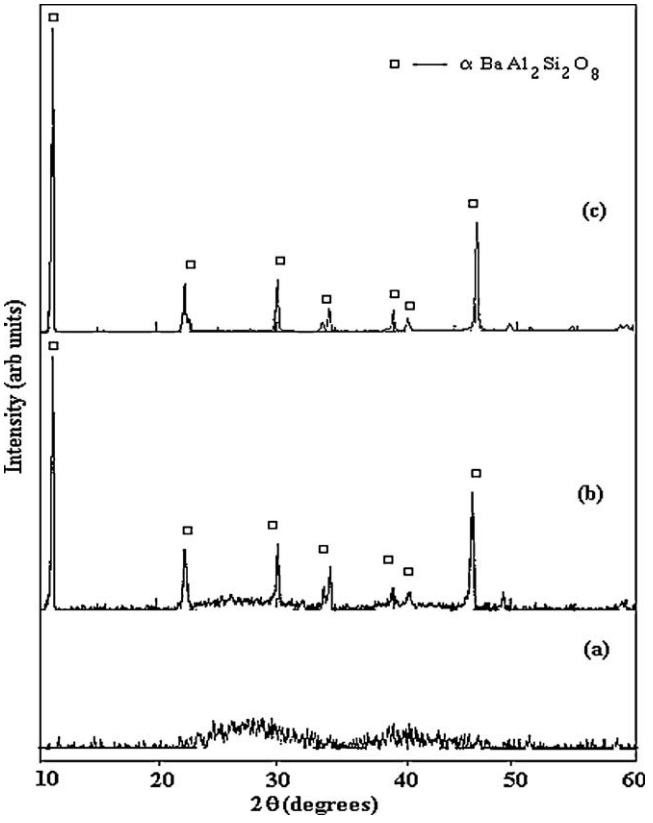

Fig. 5. XRD patterns of BAl glass (a) as prepared (b) 10 h heat treated (c) 100 h heat treated at 800 °C.

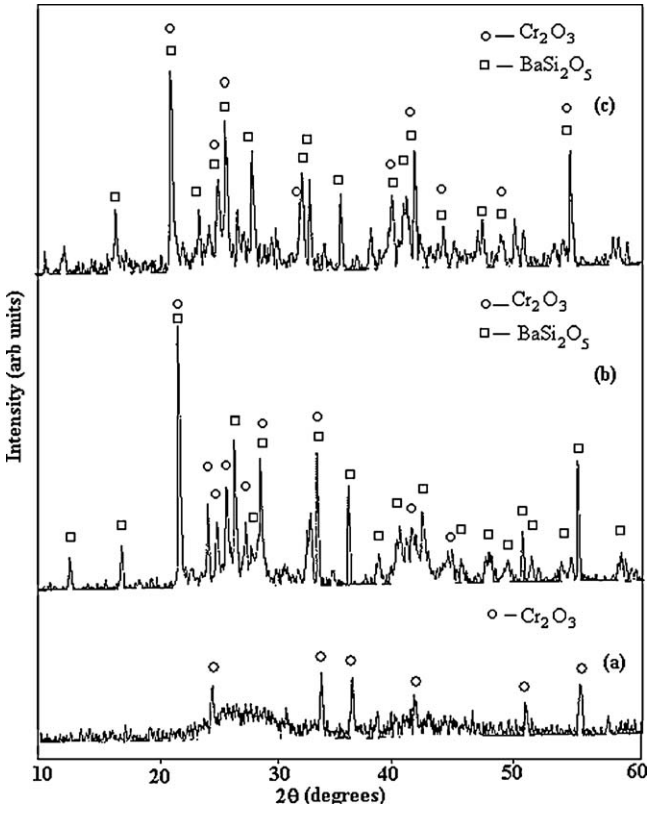

Fig. 6. XRD patterns of BCr glass (a) as prepared, (b) 10 h heat treated and (c) 100 h heat treated at 800 °C.

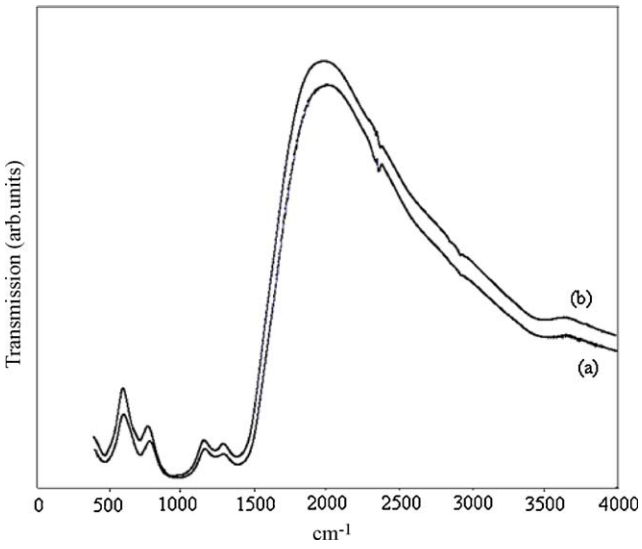

Fig. 7. FTIR spectra of BaY glass (a) as prepared and (b) 100 h heat treated at 800 °C.

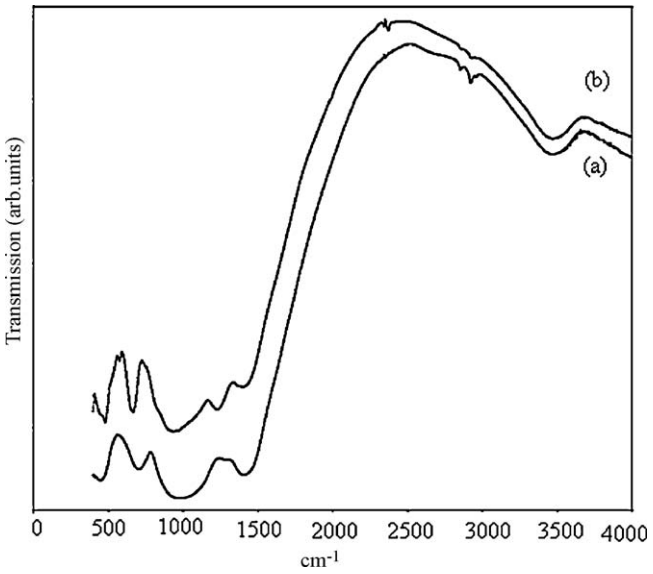

Fig. 9. FTIR spectra of BaAl glass (a) as prepared and (b) 100 h heat treated at 800 °C.

However, after heat treatment the diffused bands become sharp with splitting. This change in bands might be associated with definite crystalline phases [21].

The bands in the 300–600 cm^{-1} region are due to bending vibrations of Si–O–Si linkages. The transmittance band in the 650–800 cm^{-1} region in the glasses is attributed to the bending vibrations of bridging oxygen between trigonal boron atoms and it is also related to the stretching vibrations of the A–O bonds with A^{3+} ions in four-fold coordination (A = Y, Cr, La, Al) [24]. The band in the region 1350–1500 cm^{-1} corresponds to B–O vibrations in BO_3 triangle. Borate glasses show two characteristic bands derived from the B–O bonds in the BO_3 triangles about 1300–1500 cm^{-1} and the BO_4 tetrahedra about 1000 cm^{-1} [25]. These bands get shifted under the influence of surrounding cations, the extent and the direction of this shift depends on the type of cation. FTIR spectra of the glasses under investigation show that in these glasses boron primarily occurs in the form of BO_3 triangles (1396 cm^{-1}). However, the presence of BO_4 tetrahedron in the glass structure cannot be neglected. Since the IR band for BO_4 tetrahedron about 1000 cm^{-1} overlaps with that of stretching vibrations of SiO_4, therefore, it could not be observed [26].

The broad band in the 800–1300 cm^{-1} is assigned to the stretching vibrations of the SiO_4 tetrahedron with different number of bridging oxygen atoms [27,28]. For heat treated glasses these bands shifts towards lower wave numbers implying towards the decrease in the connectivity of the

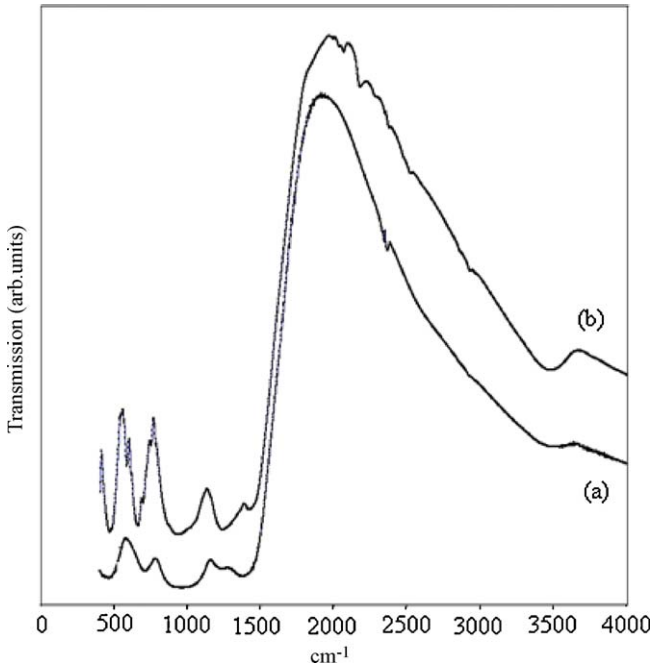

Fig. 8. FTIR spectra of BaLa glass (a) as prepared and (b) 100 h heat treated at 800 °C.

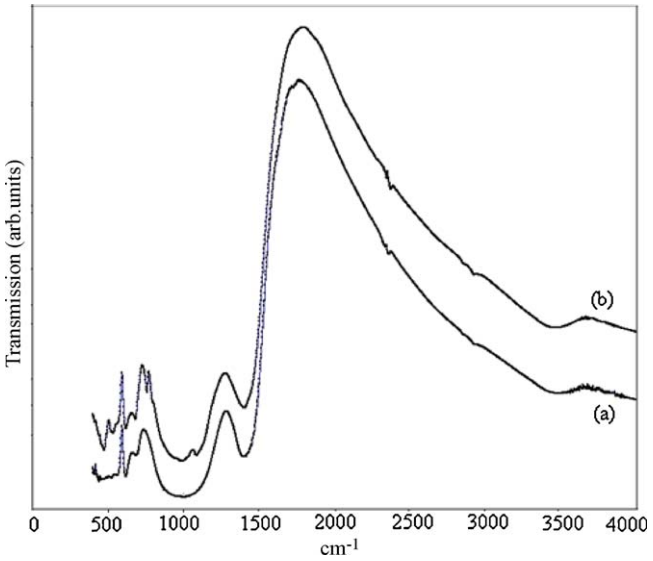

Fig. 10. FTIR spectra of BaCr glass (a) as prepared and (b) 100 h heat treated at 800 °C.

silicate glass network. The FTIR spectrum of BaY sample is shown in Fig. 7(a) and (b) for glass and glass ceramic, respectively. Glass ceramic sample shows slight change in sharpness of bands at 800–1300 cm^{-1} as compared to glass indicating small amount of rearrangement in silicate chains leading towards an ordered pattern. On the other hand, La_2O_3 containing glass as shown in Fig. 8(b), a special band centered appears at 1120–1320 cm^{-1} which is due to boroxol rings and borate stretching [21]. Apart from this, the lower wave number band (500–1000 cm^{-1}) in glass ceramics becomes sharper and split indicating that crystalline phase is formed. Similar phenomenon was also reported by Elbatal and Khalil [21].

The FTIR spectra of BaAl glass are shown in Fig. 9(a) and (b). The heat treated glass exhibit an additional band around 1200 cm^{-1} which is due to hexacelsian [24]. In case of BaCr glass and glass ceramic Fig. 10, both the spectra exhibit sharp bands. Additionally, a sharp peak is observed at 800 cm^{-1} in heat treated samples which is due to SiO_4 tetrahedron indicating presence of barium silicate also observed in XRD study. In all the four samples, the BaY and BaCr could not show any appreciable change in the FTIR spectra of glass and glass ceramics except higher sharpness of bands in heat treated sample. Obviously, there is not too much change in the basic units on the other hand BaLa and BaAl sample show remarkable differences in glass and glass ceramic due to regrouping in Si–O–Si and BO_4 structure. Additionally, the shift of the bands at lower wave number in glass ceramic also indicates that these systems have more stability than their glass counterpart.

3.4. Thermal expansion coefficient (TEC)

The BaLa glass has the highest TEC value among all the studied glasses in present investigation as shown in Table 2. The higher TEC in this glass as compared to other glasses can be associated with the higher ionic radii of La^{3+}. After heat treatment when it turns into glass ceramic the TEC value increases, which is due to the formation of crystalline phases which improve the TEC of this glass. BaY glass does not show much variation in TEC with heat treatment as very limited amount of crystallization takes place in this glass which indicates that glass matrix has undergone very little structural rearrangement. The formation of hexacelsian phase, which has a relatively higher TEC value of $\sim 8 \times 10^{-6}\ K^{-1}$ [28] greatly improves the TEC of BaAl glass after heat treatment. The change in TEC after heat treatment of this glass is observed around 10%. In case of BaCr the as prepared glass was already in crystalline form and its TEC has low value of $6.8 \times 10^{-6}\ K^{-1}$. However, after heat treatment for 10 h the crystallization of $BaSi_2O_5$ in the glass matrix increased the TEC value ($7.6 \times 10^{-6}\ K^{-1}$). With further increase in volume fraction of $BaSi_2O_5$ phase due to 100 h heat treatment the TEC value again increased to $8.1 \times 10^{-6}\ K^{-1}$. In this sample, formation of $BaSi_2O_5$ phase might be having high TEC which leads to higher % change in TEC. It might also be attributed that crystalline phase ($BaSi_2O_5$) do not exhibit the intermediate cations which may be responsible for low change in TEC due to small ionic radii as compared to the Ba^{2+} (1.49 Å).

The maximum value of TEC was recorded after 100 h heat treatment of the glasses. These heat treated glass ceramics had TEC in the range of 7.67–$8.10 \times 10^{-6}\ K^{-1}$ which is lower than Crofer ($11.5 \times 10^{-6}\ K^{-1}$). However, it is close to the permissible limit required for SOFC operation (9–$12 \times 10^{-6}\ K^{-1}$) [15,22].

Table 2
TEC of Glass and Glass ceramic after 10 and 100 h heat treatment.

Sample name	TEC (10^{-6}/K) Glass (RT to T_g)	TEC (10^{-6}/K) Glass ceramic 10 h (RT to 650 °C)	TEC (10^{-6}/K) Glass ceramic 100 h (RT to 650 °C)	% Change in TEC after 100 h heat treatment
BaY	7.58	7.69	7.80	3
BaLa	7.71	7.67	8.10	5
BaAl	6.98	7.81	7.67	10
BaCr	6.84	7.57	8.08	18

3.5. Interaction study

The BaCr sample exhibit Cr_2O_3 crystalline phase as shown in Fig. 6(a). The DTA curve of this sample could not show any clear cut endothermic peak. Therefore, this sample was heat treated around (T_c) i.e. 1000 °C for 1 h to study the change in crystallinity. The SEM microphotograph of BaCr glass heat treated at 1000 °C for 1 h is shown in Fig. 11. It can be clearly seen that after heat treatment for 1 h, some crystals grow as small floral patterns embedded in glass matrix. These floral patterns have been formed by combination of small needle shaped crystals of barium silicate phase as reported by Bansal and Gamble [28]. This sample showed highest change in TEC after 100 h heat treatment at 800 °C. Moreover, due to the presence of Cr_2O_3 in glass as well as in Crofer 22 APU this

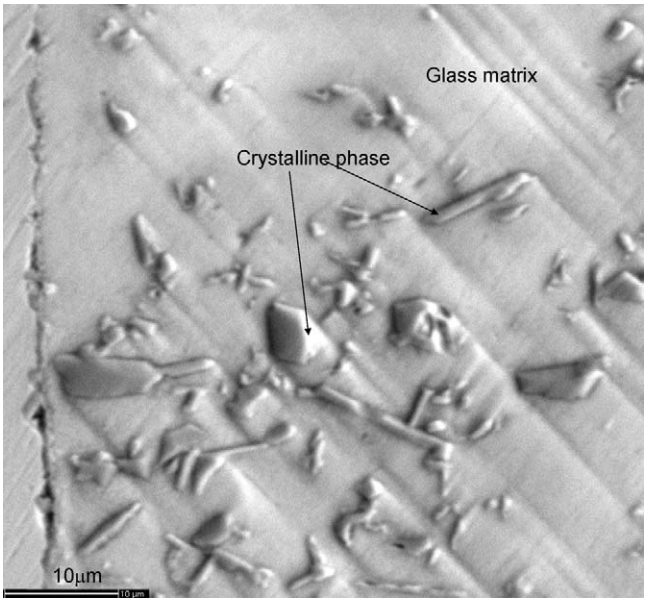

Fig. 11. Microstructure (SEM) of BaCr glass heat treated at 1000 °C for 1 h showing microcrystalline floral pattern of barium silicate.

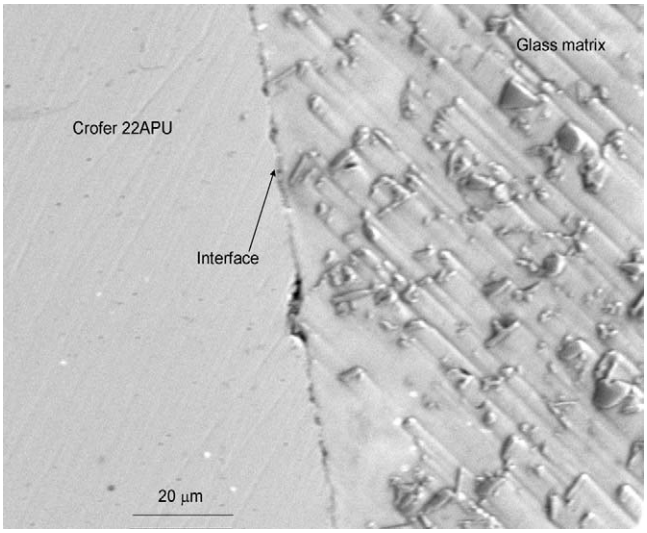

Fig. 12. Microstructure (SEM) of interface between Crofer 22 APU and BaCr glass developed after 1 h heat treatment at 1000 °C.

glass was selected to study its bonding characteristics with Crofer 22 APU. A highly uniform and homogenous interface is formed as indicated in Fig. 12. However, the small voids of the order of few micrometers, which are visible in the micrograph, are due to chipping out of glass during grinding and polishing while preparation of sample for SEM. Preliminary studies clearly indicate good adhesion without any gap at the interface. Based on preliminary results, the compatibility study was extended for 20 h to study the growth of interface by elemental analysis as shown in Fig. 13 and Table 3. The interface is devoid of any cracks and with the increase of heat treatment time it

Table 3
Elemental analysis at the BaCr glass and Crofer interface.

Element	Weight [%]	Error [%]
Fe	63.74	1.7
Au	8.46	1.0 (coating)
Cr	21.73	0.6
C	5.69	0.3
Ba	0.38	0.1

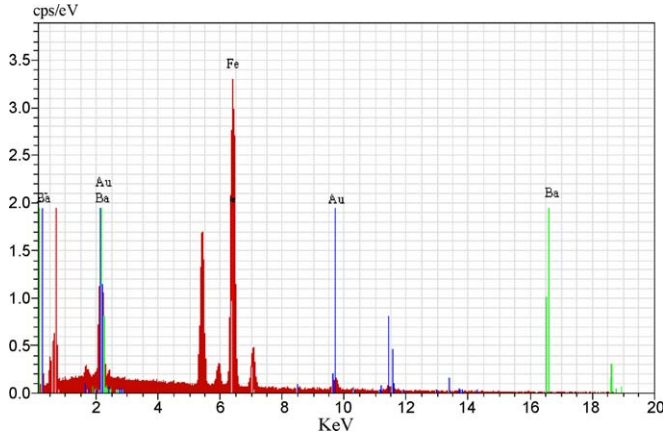

Fig. 14. Elemental analysis at the point marked in the interface between Crofer 22 APU and BaCr glass.

becomes smoother and shows good adherence to the Crofer. The major elements present at the interface are Fe, Cr and Ba. The interdiffusion of Fe and C from the Crofer and Ba from the glass took place at the interface whereas Cr interdiffused from the glass as well as the Crofer. However, Si was not present at

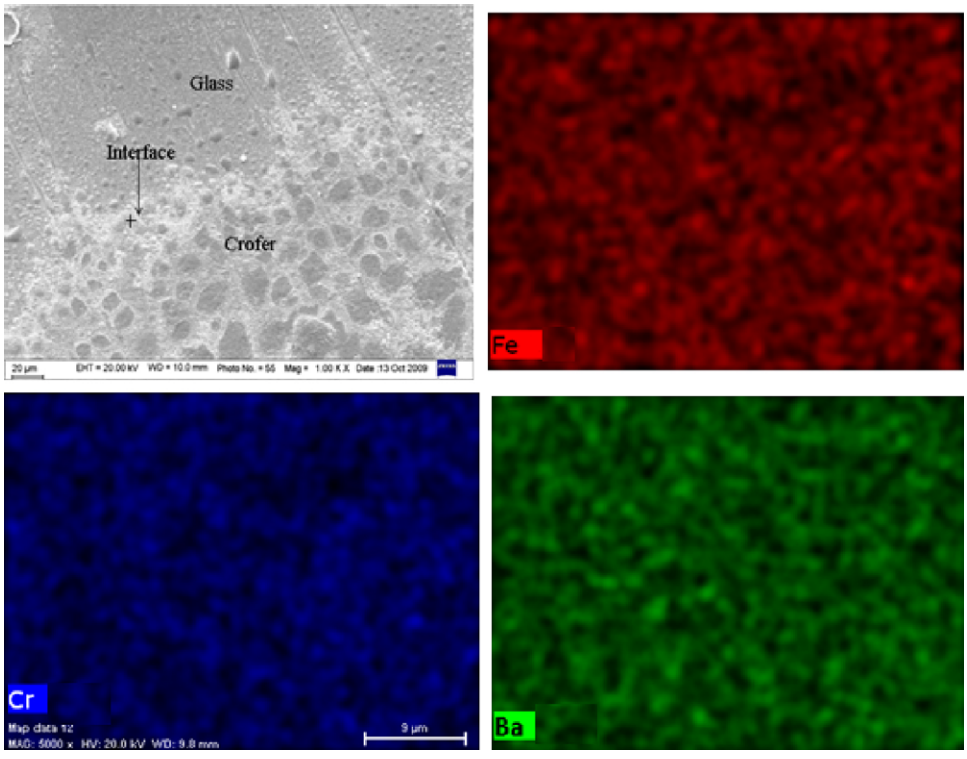

Fig. 13. Microstructure (SEM) of interface between Crofer 22 APU and BaCr glass developed after 20 h heat treatment at 1000 °C along with X-ray dot mapping.

the interface (as shown by point elemental analysis in Fig. 14) which means it could not diffuse out from the glass matrix.

4. Conclusions

BaY glass shows higher glass transition (T_g) temperature with higher stability than BaAl and BaLa glasses. The TEC value of BaY, BaLa, BaAl glass ceramics was observed to be higher than their glass counterparts due to formation of crystalline phases. The change in TEC depends on the fraction of crystalline phase in the glass matrix and its chemical nature and structure. The FTIR spectra of glass ceramics exhibit sharp and split transmission bands as compared to parent glass. After heat treatment at 800 °C for 100 h, no detrimental crystalline phase is observed for SOFC application. Formation of hexacelsian phase after heat treatments in BaAl glass has improved its TEC bringing it close to the required limit for SOFC application. BaY glass composition could be used a sealant material because of limited or no crystallization even after 100 h heat treatment and suitable value of TEC.

Acknowledgement

The financial support provided by Department of Science and Technology (DST), Govt. of India, under the scheme SR/S2/CMP-48/2004 is greatly acknowledged.

References

[1] ZhenguoYang, Guanguang Xia, Kerry D. Meinhardt, K. ScottWell, Jeff W. Stevenson, Chemical stability of glass seal interfaces in intermediate temperature solid oxide fuel cells, J. Mater. Eng. Perform. 13 (3) (2004) 327–334.
[2] N.Q. Minh, Solid oxide fuel cell technology features and applications, Solid State Ionics 174 (2004) 271–277.
[3] S.C. Singhal, Solid oxide fuel cells for stationary, mobile and military applications, Solid State Ionics 152–153 (2003) 405–410.
[4] N.Q. Minh, Ceramic fuel cells, J. Am. Ceram. Soc. 76 (3) (1993) 563–588.
[5] B.C.H. Steele, A. Heinzel, Materials for fuel-cell technologies, Nature 414 (6861) (2001) 345–352.
[6] S.P.S. Badwal, Stability of solid oxide fuel cell components, Solid State Ionics 143 (1) (2001) 39–46.
[7] L.J. Gauckler, D. Beckel, B.E. Buergler, E. Jud, U.P. Muecke, M. Prestat, J.L.M. Rupp, J. Richter, Solid oxide fuel cells, Syst. Mater. Chim. 58 (12) (2004) 837–850.
[8] C. Lara, M.J. Pascual, A. Duran, Glass-forming ability sinterability and thermal properties in the systems RO-BaO-SiO_2 (R = Mg, Zn), J. Non-Cryst. Solids 348 (2004) 149–155.
[9] C. Lara, M.J. Pascual, R. Keding, A. Duran, Electrical behaviour of glass-ceramics in the systems RO-BaO-SiO_2 (R = Mg, Zn) for sealing SOFCs, J. Power sources 157 (2006) 377–384.
[10] N. Lahl, K. Singh, L. Singheiser, K. Hilpert, Crystallisation kinetics in AO-Al_2O_3-SiO_2-B_2O_3 glasses (A = Ba, Ca, Mg), J. Mater. Sci. 35 (2000) 3089–3096.
[11] S.-B. Sohn, S.-Y. Choi, G.-H. Kirr, H.-S. Song, G.-D. Kim, Suitable glass-ceramic sealant for planar solid-oxide fuel cells, J. Am. Ceram. Soc. 87 (2) (2004) 254–260.
[12] Jeffrey W. Fergus, Sealants for solid oxide fuel cells, J. Power sources 147 (2005) 46–47.
[13] K. Singh, N. Gupta, O.P. Pandey, Effect of Y_2O_3 on the crystallization of SiO_2-MgO-B_2O_3-Al_2O_3 glasses, J. Mater. Sci. 42 (2007) 6426.
[14] A. Arora, E.R. Shaaban, K. Singh, O.P. Pandey, Non-isothermal crystallization kinetics of ZnO–BaO–B_2O_3–SiO_2 glass, J. Non-Cryst. Solids 354 (33) (2008) 3944.
[15] C. Lara, M.J. Pascual, M.O. Prado, A. Durán, Sintering of glasses in the system RO–Al_2O_3–BaO–SiO_2 (R = Ca, Mg, Zn) studied by hot-stage microscopy, Solid State Ionics 170 (2004) 201–208.
[16] V. Kumar, S. Sharma, O.P. Pandey, K. Singh, Thermal and physical properties of 30SrO-40SiO_2-20B_2O_3-10A_2O_3 (A = La, Y, Al) glasses and their chemical reaction with bismuth vanadate for SOFC, Solid State Ionics 181 (2010) 79–85.
[17] N.H. Ray, Composition-property relationships in ionorganic oxide glasses, J. Non-Cryst. Solids 15 (1974) 423–434.
[18] H.S. Chen, A method for evaluating viscosities of metallic glasses from the rates of thermal transformations, J. Non-Cryst. Solids 27 (1978) 257.
[19] J.A. Macmillan, Crystallization kinetics in new Sb As Se Te amorphous glasses, J. Phys. Chem. 42 (1965) 3497.
[20] V. Kumar, A. Arora, O.P. Pandey, K. Singh, Studies on thermal and structural properties of glasses as sealants for solid oxide fuel cells, Int. J. Hydrogen Energy 33 (1) (2008) 434.
[21] F.H.A. Elbatal, M.M.I. Khalil, Gamma rays interaction with ternary silicate glasses containing mixed CoO + NiO, Mater. Chem. Phys. 82 (2) (2003) 375.
[22] M.K. Mahapatra, K. Lu, R.J. Bodnar, Network structure and thermal property of a novel high temperature seal glass, Appl. Phys. A 95 (2009) 493–500.
[23] S. Ghosh, P. Kundu, A. Das Sharma, R.N. Basu, H.S. Maiti, Microstructure and property evaluation of barium aluminosilicate glass–ceramic sealant for anode-supported solid oxide fuel cell, J. Eur. Ceram. Soc. 28 (2008) 69–76.
[24] A. Goel, D.U. Tulyaganov, E.R. Shabaan, C.S. Knee, S. Eriksson, J.M.F. Ferreira, Structure and crystallization behaviour of some $MgSiO_3$-based glasses, Acta Mater. 56 (13) (2008) 3065.
[25] L. Stoch, M. Sroda, Infrared spectroscopy in the investigation of oxide glasses structure, J. Mol. Struct. 77–84 (1999) 511–512.
[26] S.-L. Lin, C.S. Hwang, Structures of CeO_2-Al_2O_3–SiO_2 glasses, J. Non-Cryst. Solids 202 (1996) 61–67.
[27] J.T. Kohli, J.E. Shelby, J.S. Frye, A structural investigation of yttrium aluminosilicate glasses using Si-29 and Al-27 magic angle spinning nuclear-magnetic-resonance, Phys. Chem. Glasses 33 (1992) 73–78.
[28] N.P. Bansal, E.A. Gamble, Crystallization kinetics of a solid oxide fuel cell seal glass by differential thermal analysis, J. Power Sources 147 (2005) 107–115.